Roadless Space of the Conterminous United States
Raymond D. Watts, *et al.*
Science **316**, 736 (2007);
DOI: 10.1126/science.1138141

Science (print ISSN 0036-8075; online ISSN 1095-9203) is published weekly, except the last week in December, by the American Association for the Advancement of Science, 1200 New York Avenue NW, Washington, DC 20005.

Roadless Space of the Conterminous United States

Raymond D. Watts,[1]* Roger W. Compton,[2] John H. McCammon,[2] Carl L. Rich,[2] Stewart M. Wright,[2] Tom Owens,[2] Douglas S. Ouren[1]

Roads encroaching into undeveloped areas generally degrade ecological and watershed conditions and simultaneously provide access to natural resources, land parcels for development, and recreation. A metric of roadless space is needed for monitoring the balance between these ecological costs and societal benefits. We introduce a metric, roadless volume (RV), which is derived from the calculated distance to the nearest road. RV is useful and integrable over scales ranging from local to national. The 2.1 million cubic kilometers of RV in the conterminous United States are distributed with extreme inhomogeneity among its counties.

The road network of the United States exceeds 6.3 million km in aggregate length (*1*) and fills the national landscape so fully that, except in Alaska, one can get no farther from a road than 35 km (*2*). This extensive road network provides societal benefits by bringing natural resources to consumers, linking workers to jobs, and connecting people to urban services. It is in the spaces between the roads that valuable natural resources are present and ecosystem services are rendered. Road encroachment affects ecological resources, primarily in negative ways (*1*, *3*–*8*), usually by fragmenting habitats and introducing chemical contaminants and exotic species to the ecosystem. Roads have been demonstrated to have dozens, if not hundreds, of effects on ecosystems and watersheds (*1*, *3*–*5*, *7*–*11*). Physical, chemical, and biological processes transmit influences from roads to their surroundings in a mélange of deterministic, stochastic, and chaotic processes that are made even more complex through their interactions with the variability of the landscape. The span of documented effects ranges from a few meters to many kilometers (*1*) and depends not only on the roads themselves but also on the volume and types of traffic that they carry. These complexities make it impractical to measure or estimate the area of influence without extensive local observation. Our work is aimed at bridging these details in order to answer two questions: (i) how much space is there between the roads, and (ii) how much is lost as new roads are added to the network, penetrating roadless space? These questions cannot be answered by measuring either the length or surface area of roads because these metrics do not respond to road placement. We sought a metric that would have a greater response to a road penetrating deeply into otherwise roadless space than to a road of similar length lying close to other roads.

We introduce a metric called roadless volume (RV). RV calculation begins with the computation of the horizontal distance to the nearest road (DTR), which is most accurately done with fast-marching methods (*12*) or adequately done with network methods (*13*); the network computation method is available in many geographic information systems. In practice, DTR is computed for points on a square grid (we used a 30-m grid); grid size does not bias results, but it affects accuracy. RV for an area is the integral of DTR over the area, which is estimated to be the total of the DTR cell values multiplied by cell area, with resulting units of cubic meters or cubic kilometers. Calculation accuracy depends on cell size, the quality of the road data set used for DTR computation, the sinuosity of roads, and (to a small degree) the method of calculation. RV is objective; there are no arbitrary factors.

RV can be described and visualized as follows: Substitute DTR for elevation to create a pseudotopographic surface (real topography plays no role in our definition of RV). RV of a footprint area is the volume of the pseudotopography above that footprint (Fig. 1). Roads of equal length produce different RV changes, depending on their alignments with respect to other roads (Fig. 2). RV responds simultaneously to footprint area, footprint shape, and the alignment of roads within the footprint. Compact footprints with no internal roads produce maximum RV. Meandering boundaries and internal roads diminish RV. The greatest reduction comes from roads that penetrate places that otherwise would be most remote from roads. Roads placed close to other roads only modestly reduce RV.

We calculated DTR for the entire United States on a 30-m grid aligned with the National Land Cover Dataset (NLCD), thus enhancing a national geospatial resource that is used for a wide variety of ecological and land-use analyses (*6*, *14*, *15*). RV for any footprint is $A\langle DTR\rangle$, where A is the area of the footprint and $\langle DTR\rangle$ is its mean DTR. With this definition, footprints need not be bounded by roads, enabling calculations of RV for counties (*16*). By summing county RV values, we estimated the RV of the conterminous United States to be 2.1×10^6 km^3. Maps inherently provide visual weighting by area, so we color-coded county results (Fig. 3) by $\langle DTR\rangle$ values rather than by RV, thus avoiding double emphasis of county size.

Roadless space is an asset that is unequally distributed by county and further unequally distributed among the population. Residents of two counties with equal RV have different per-capita shares of the roadless-space resource in inverse proportion to the county populations. Figure 4 shows per-capita RV by county, which can also be interpreted as the pressure of population against the counties' roadless spaces. Comparing Figs. 3 and 4, one sees that some counties with high DTR, and therefore high RV, have low per-capita RV. Prominent examples occur on the Pacific coast, along the Wasatch Front in Utah, along the Front Range in Colorado, and at the southern tips of Nevada and Florida; all these counties have metropolitan areas closely juxtaposed with mountains, deserts, or (in Florida) extensive wetlands. In contrast, low county populations create high per-capita RV in a band of counties stretching from the Dakotas to western Texas, in spite of relatively low DTR in most of these counties.

The county with the lowest per-capita RV is Kings County in New York (Brooklyn; roughly 4000 m^3 per capita, giving each person the equivalent of a 45° pyramid that is 30 m long on a side) (*17*), and the county with the highest per-

Fig. 1. RV is calculated by substituting DTR for elevation and then calculating the volume beneath the pseudotopographic surface. Two examples are shown, with perimeter roads in blue (there is a hidden road along the back of each volume). (**Left**) For a 1-km-square road pattern, the pyramid has a height of 0.5 km and a volume of 0.167 km^3. (**Right**) The elongated pyramid measures 0.333 by 3 km and therefore has the same footprint area as the square pyramid, but its volume is 47% of the square pyramid volume. RV simultaneously accounts for area and shape.

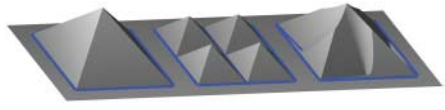

Fig. 2. (**Left**) A square road pattern produces a pyramid of roadless volume. (**Center**) Four added roads, each of length = 0.5 × (the length of one pyramid side) and intersecting at the center (the two roads parallel to the long side of the image are mostly hidden), reduce the pyramid volume by 50%. (**Right**) Four roads of the same length, starting at the corners and angled slightly toward the center (tan divergence angle = 0.1), diminish the pyramid volume by only 13.5%.

[1]U.S. Geological Survey (USGS), Fort Collins, CO 80526-8118, USA. [2]USGS, Denver, CO 80225-0046, USA.

*To whom correspondence should be addressed. E-mail: rwatts@usgs.gov

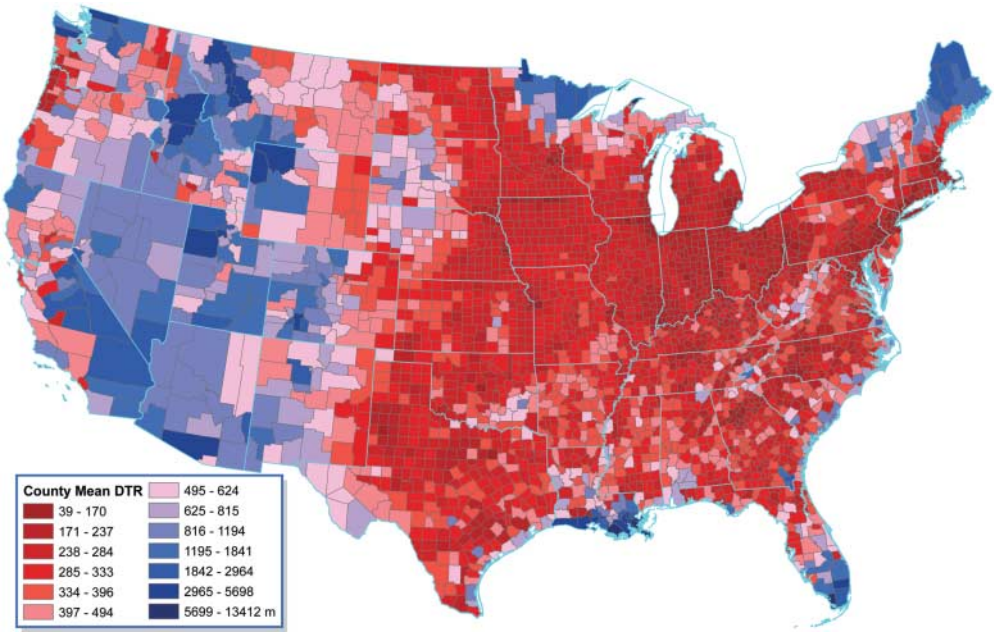

Fig. 3. Map of <DTR> by county in the conterminous United States. DTR legend classes are of approximately equal area, and color rendering closely follows area-adjusted county rank.

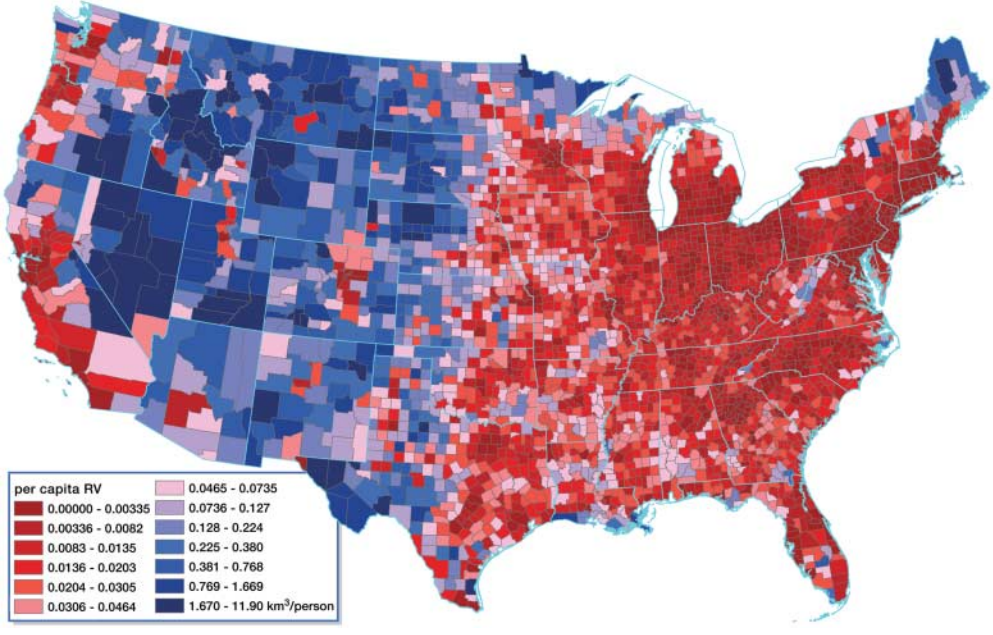

Fig. 4. Per-capita RV by county for the conterminous United States. Legend classes are of approximately equal area, and color rendering closely follows area-adjusted county rank.

capita RV is Hinsdale County in southern Colorado (11.9 km^3 per capita, giving each person a pyramid that is 4.1 km long on a side). The contrast in ecological conditions between these counties is extreme: One county is a dense urban area; the other is largely wilderness. The ratio of least to greatest roadless space per person in the conterminous United States, measured at the county scale, is approximately $1:3 \times 10^6$: a greater dynamic range than that of other common socioeconomic statistics at the county scale, such as population density ($1:7 \times 10^5$) (*18*) or mean income (1:7.8) (*19*). This large dynamic range implies that counties with low population densities also have few roads, large values of <DTR>, and large RV.

Socioeconomic processes add roads, diminishing DTR and RV. An assessment of changes in RV requires detailed and consistent maps on multiple dates, which are available in only a few places. One such place is the Front Range in Colorado, for which we made a movie of the change of RV from 1937 to 1997 (*20*). Here, nearly half of the initial RV was lost during the 60-year study period, as a result of urban expansion, growth of small towns, and housing dissemination—all occurring on agricultural land.

It is reasonable to postulate that distance from roads, on average, diminishes road influences, an application of a geographic law introduced by Tobler (*21*). Thus, although we cannot trace the details of road-induced effects, it may nevertheless be useful to know the extent to which we are diminishing the space where these effects are least likely and least intense. RV is a sensitive indicator that summarizes the status of this space.

References and Notes

1. R. T. T. Forman *et al.*, *Road Ecology: Science and Solutions* (Island Press, Washington, DC, 2003).
2. There are other places that are more remote from roads on islands and in Louisiana coastal swamps. The 35-km landlocked maximum distance occurs in Wyoming, near the southeast corner of Yellowstone National Park.
3. D. G. Havlick, *No Place Distant: Roads and Motorized Recreation on America's Public Lands* (Island Press, Washington, DC, 2002).
4. S. C. Trombulak, C. A. Frissell, *Conserv. Biol.* **14**, 18 (2000).

5. R. T. T. Forman, R. D. Deblinger, *Conserv. Biol.* **14**, 36 (2000).
6. K. H. Riitters, J. D. Wickham, *Front. Ecol. Environ.* **1**, 125 (2003).
7. R. T. T. Forman, L. E. Alexander, *Annu. Rev. Ecol. Syst.* **29**, 207 (1998).
8. J. L. Gelbard, J. Belnap, *Conserv. Biol.* **17**, 420 (2003).
9. R. L. DeVelice, J. R. Martin, *Ecol. Appl.* **11**, 1008 (2001).
10. I. F. Spellerberg, *Ecological Effects of Roads, Land Reconstruction and Management* (Science Publishers, Enfield, NH, 2002).
11. A. C. Yost, R. G. Wright, *Arctic* **54**, 41 (2001).
12. J. A. Sethian, *Level Set Methods and Fast Marching Methods: Evolving Interfaces in Computational Geometry, Fluid Mechanics, Computer Vision, and Materials Science* (Cambridge Univ. Press, Cambridge, ed. 2, 1999).
13. E. W. Dijkstra, *Numer. Math.* **1**, 269 (1959).
14. H. John Heinz III Center for Science, Economics, and the Environment, *The State of the Nation's Ecosystems: Measuring the Lands, Waters, and Living Resources of the United States* (Cambridge Univ. Press, Cambridge, 2002).
15. C. Homer, M. Coan, C. Huang, L. Yang, B. Wylie, *Photogramm. Eng. Remote Sens.* **70**, 829 (2004).
16. Materials and methods, including a table of county values of mean DTR and RV, are available as supporting material on *Science* Online.
17. Because calculations were done with a 30-m grid, the accuracy of the calculations is low where roads are dense. The approximate RV per-capita value for Kings County in New York is provided to illustrate the great contrast with the value for Hinsdale County in Colorado.
18. Bureau of the Census, in National Atlas of the United States, 2006 (www.nationalatlas.gov).
19. Bureau of Economic Analysis, in National Atlas of the United States, 2006 (www.nationalatlas.gov).
20. The movie of RV change for the Colorado Front Range is available as supporting material on *Science* Online.
21. W. R. Tobler, *Econ. Geogr.* **46**, 234 (1970).
22. We thank the Southern Rockies Ecosystem Project for introducing us to large-area DTR maps nearly a decade ago. Support for the development and analysis of national DTR data was provided by the USGS Geographic Analysis and Monitoring Program.

Supporting Online Material

www.sciencemag.org/cgi/content/full/316/5825/736/DC1
Materials and Methods
SOM Text
Tables S1 and S2
References
Movie S1

29 November 2006; accepted 22 March 2007
10.1126/science.1138141

Pyroclastic Activity at Home Plate in Gusev Crater, Mars

S. W. Squyres,[1] O. Aharonson,[2] B.C. Clark,[3] B. A. Cohen,[4] L. Crumpler,[5] P. A. de Souza,[6] W. H. Farrand,[7] R. Gellert,[8] J. Grant,[9] J. P. Grotzinger,[2] A. F. C. Haldemann,[10] J. R. Johnson,[11] G. Klingelhöfer,[12] K. W. Lewis,[2] R. Li,[13] T. McCoy,[14] A. S. McEwen,[15] H. Y. McSween,[16] D. W. Ming,[17] J. M. Moore,[18] R. V. Morris,[17] T. J. Parker,[10] J. W. Rice Jr.,[19] S. Ruff,[19] M. Schmidt,[14] C. Schröder,[12] L. A. Soderblom,[11] A. Yen[10]

Home Plate is a layered plateau in Gusev crater on Mars. It is composed of clastic rocks of moderately altered alkali basalt composition, enriched in some highly volatile elements. A coarse-grained lower unit lies under a finer-grained upper unit. Textural observations indicate that the lower strata were emplaced in an explosive event, and geochemical considerations favor an explosive volcanic origin over an impact origin. The lower unit likely represents accumulation of pyroclastic materials, whereas the upper unit may represent eolian reworking of the same pyroclastic materials.

Home Plate is a light-toned plateau ~90 m in diameter and 2 to 3 m high within the Inner Basin of the Columbia Hills, at Spirit's landing site in Gusev crater (*1*–*3*). Home Plate appears prominent from orbit, and was identified after landing as a high-priority target. It is the most extensive exposure of layered bedrock encountered by Spirit at Gusev to date.

Spirit arrived at the northern edge of Home Plate on sol 744 (*4*), following the path shown in Fig. 1. Images of the plateau show a thick stack of layered rocks, with a lower coarse-grained unit and an upper finer-grained unit (Fig. 2). The lower unit is characterized by prominent parallel layering with low apparent dips and a coarse granular texture (Fig. 2B). Individual granules are roughly equant, and typically 0.5 to 3 mm in size. It is difficult to determine in Microscopic Imager (MI) images whether the granules are original clasts, such as accretionary lapilli, or textures reflecting postdepositional cementation (fig. S1). Toward the top of the lower unit is a massive section roughly 10 cm thick where layering becomes indistinct (Fig. 3) and grains are difficult to identify in MI images (fig. S2).

A particularly notable feature in the lower unit is a ~4-cm clast with deformed layers beneath it, interpreted to be a bomb sag (Fig. 3). Bomb sags are found in volcaniclastic deposits on Earth, where outsized clasts ejected from an explosive vent are emplaced ballistically into deformable materials, causing downward deflection of layering.

In contrast to the lower unit, the upper unit is fine grained, well sorted, and finely laminated, and it exhibits cross-stratification. On the northern edge of Home Plate, the upper unit exposes a facies that is well bedded and characterized by ubiquitous fine lamination that is arranged in bed sets with planar to low-angle cross-stratification (Fig. 2C). Other features of this facies include gently dipping curved or irregular surfaces of erosion, small-scale cut-and-fill structures, convex-upward laminations, and occasional intercalation of thin beds of high-angle cross-bedding. In MI images, this facies exhibits a distinctly clastic texture, with grains 200 to 400 μm in diameter that are exceptionally well rounded and sorted (fig. S3).

A second facies in the upper unit that is particularly well developed at the eastern edge of Home Plate exhibits high-angle cross-bedding (Fig. 4). Here, the geometry is expressed as wedge sets up to several tens of centimeters thick of distinctly trough-shaped cross-strata. Internal stratification ranges from finely laminated to more thickly laminated. Cross-strata also preserve evidence of reactivation surfaces, cut at variable angles and generally backfilled by cross-strata concordant with the scour surface. Such geometries typically form during reconfiguration of the bed in response to scouring during flow bursting, migration of three-dimensional bedforms with frontal scour pits, and at times when the sediment concentration of a flow is decreased.

We used planar fits to bedding seen in Pancam images to estimate the structural attitudes of beds in the upper unit of Home Plate, at four locations that sample roughly a third of the plateau's perimeter (fig. S4). At all four locations, the beds dip inward toward the center of Home Plate. The 1σ range of derived dips is 5° to 20°, with occasional values up to 30°. Dips are consistent within each outcrop, suggesting that the measurements reflect a true structural trend and are not greatly influenced by low-angle cross-bedding.

Chemical compositions analyzed by the Alpha Particle X-ray Spectrometer (APXS) are

[1]Department of Astronomy, Space Sciences Building, Cornell University, Ithaca, NY 14853, USA. [2]Division of Geological and Planetary Sciences, California Institute of Technology, Pasadena, CA 91125, USA. [3]Lockheed Martin Corporation, Littleton, CO 80127, USA. [4]Institute of Meteoritics, University of New Mexico, Albuquerque, NM 87131, USA. [5]New Mexico Museum of Natural History and Science, Albuquerque, NM 87104, USA. [6]Vallourec Research Center, F-59260 Aulnoye-Aymeries, France. [7]Space Science Institute, Boulder, CO 80301, USA. [8]Department of Physics, University of Guelph, Guelph, ON, N1G 2W1, Canada. [9]Center for Earth and Planetary Studies, Smithsonian Institution, Washington, DC 20560, USA. [10]Jet Propulsion Laboratory, California Institute of Technology, Pasadena, CA 91109, USA. [11]United States Geological Survey, Flagstaff, AZ 86001, USA. [12]Institut für Anorganische und Analytische Chemie, Johannes Gutenberg-Universität, Mainz, Germany. [13]Department of Civil and Environmental Engineering and Geodetic Science, Ohio State University, Columbus, OH 43210, USA. [14]Department of Mineral Sciences, National Museum of Natural History, Smithsonian Institution, Washington, DC 20560, USA. [15]Lunar and Planetary Laboratory, University of Arizona, Tucson, AZ 85721, USA. [16]Department of Earth and Planetary Sciences, University of Tennessee, Knoxville, TN 37996, USA. [17]Astromaterials Research and Exploration Science, NASA Johnson Space Center, Houston, TX 77058, USA. [18]NASA Ames Research Center, Moffett Field, CA 94035, USA. [19]Department of Geological Sciences, Arizona State University, Tempe, AZ 85287, USA.